

Foldamers

Folding-Induced Folding: The Assembly of Aromatic Amide and 1,2,3-Triazole Hybrid Helices

Chun-Fang Wu,^[a] Zhi-Ming Li,^[b] Xiao-Na Xu,^[a] Zhi-Xiong Zhao,^[a] Xin Zhao,^{*[a]}
Ren-Xiao Wang,^[a] and Zhan-Ting Li^{*[a, b]}

Abstract: Folding-induced folding for the construction of artificial hybrid helices from two different kinds of aromatic sequences is described. Linear compounds **1a**, **1b**, and **2**, containing one aromatic amide trimer or pentamer and one or two aromatic 1,2,3-triazole tetramers, have been designed and synthesized. The trimeric and pentameric amide segments are driven by intramolecular N–H...F hydrogen bonding to adopt a folded or helical conformation, whereas the triazole segment is intrinsically disordered. In organic solvents of low polarity, the amide foldamer segment induces the attached triazole segment(s) to fold through intramolecular stacking, leading to the formation of hybrid helices. The helical conformation of these hybrid sequences has been

confirmed by ¹H and ¹⁹F NMR spectroscopy, UV/Vis spectroscopy, circular dichroism (CD) experiments, and theoretical calculations. It was found that the amide pentamer exhibits a stronger ability to induce the folding of the attached triazole segment(s) compared with that of the shorter trimer. Enantiomers (*R*)-**3** and (*S*)-**3**, which contain an *R*- or *S*-(1-naphthyl)ethylamino group at the end of a tetraamide segment, have also been synthesized. CD experiments showed that introduction of a chiral group caused the whole framework to produce a strong helicity bias. Density-functional-theory calculations on (*S*)-**3** suggested that this compound exists as a right-handed (*P*) helix.

Introduction

The complicated functions of proteins rely on their three-dimensional (3D) structures, which consist of different local secondary structures such as α -helices, β -sheets, and β -turns. In most cases, these secondary structures are stabilized by intramolecular hydrogen-bonding, aromatic-stacking, and hydrophobic interactions.^[1] However, these secondary structures may also be induced through binding to ordered structures or higher-grade partners.^[2] In this manner, nature has developed molecular chaperones,^[3] which are proteins that can assist intrinsically disordered proteins to fold. Moreover, many biomacromolecules, such as glycoproteins^[4] and nucleoproteins,^[5] are composed of two or more sequences of discrete repeating units. These different segments interact with each other and cause the molecule to produce well-defined 3D ordered structures and functions. Given the importance of these biomacro-

molecules in life, it would be of value to design synthetic systems that can mimic their advanced structures and functions.

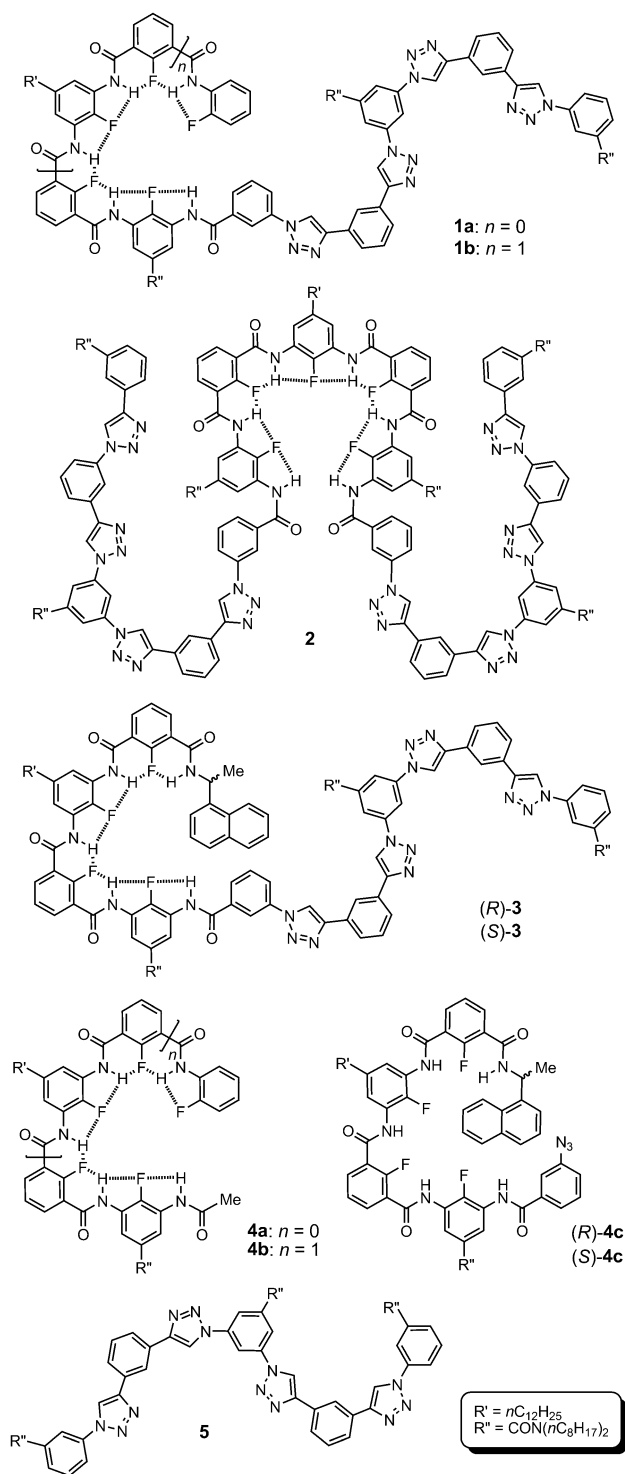
Recently, there has been much interest in creating foldamers that can mimic the ability of biomacromolecules, particularly peptides and proteins, to fold into well-defined conformations.^[6–23] Currently, a variety of secondary-structure sequences consisting of repeat units is being developed. Examples of supersecondary, tertiary, and quaternary structures, containing two or more segments possessing a secondary structure, have also been reported.^[24–30] Many of these synthetic systems have applications in molecular recognition,^[8–10, 19–23] catalysis,^[31–33] design of functional materials,^[34] and bioactive molecules.^[35, 36] The properties of both natural and synthetic systems are closely related to their sequences and structures. Therefore, the development of efficient strategies to construct new compact backbones could provide the opportunity to further extend the functions and applications of synthetic systems. The choice of noncovalently tunable molecular units that can be used to construct repeat sequences is limited; however, a promising strategy is to construct hybrid frameworks by combining different types of repeat unit into one entity. To realize this, the covalently connected units would need to be able to produce specific noncovalent interactions, such that the whole molecule can self-assemble into a defined compact structure.

Aromatic amide foldamers that result from hydrogen bonding represent a large family of synthetic secondary structures.^[23b] Although intramolecular N–H...N and N–H...O hydrogen bonds are typically used to encourage folded conformations,^[13a, 23b] we found that N–H...F hydrogen bonds are also

[a] Dr. C.-F. Wu, Dr. X.-N. Xu, Dr. Z.-X. Zhao, Prof. Dr. X. Zhao, Prof. Dr. R.-X. Wang, Prof. Dr. Z.-T. Li
Shanghai Institute of Organic Chemistry, Chinese Academy of Sciences
345 Lingling Lu, Shanghai 200032 (China)
Fax: (+86) 21-64166128
E-mail: ztli@mail.sioc.ac.cn
xzhao@mail.sioc.ac.cn

[b] Dr. Z.-M. Li, Prof. Dr. Z.-T. Li
Department of Chemistry, Fudan University
220 Handan Road, Shanghai 200433 (China)

Supporting information for this article is available on the WWW under <http://dx.doi.org/10.1002/chem.201304161>.



strong enough to encourage aromatic oligoamides to form folded conformations.^[37] Because fluorine atoms do not produce as much steric hindrance as the widely used alkoxy groups, N–H...F hydrogen-bonded amide foldamers possess a high degree of planarity and consequently, a high stacking propensity.^[38–40] In recent years, a series of alternating 1,2,3-triazole and benzene or pyridine oligomers have also been demonstrated to form helical conformations, driven by intermolecular C–H...Cl[−] hydrogen bonding,^[41–44] hydrophobicity,^[45] or in-

tramolecular C–H...O hydrogen bonding.^[46,47] The backbone of these oligomers is conformationally disordered, but the C–H...Cl[−] hydrogen-bonding-induced helical conformations have a diameter comparable to that of the N–H...F hydrogen bonded amide foldamers. Thus, we envisioned that an intrinsically folded aromatic oligoamide might induce one or two covalently connected and intrinsically disordered triazole oligomers to fold by means of strong intramolecular stacking, leading to the formation of new hybrid helices. Huc and Tanatani and co-workers have reported that folded 8-amino-2-quinoline-carboxylic acid oligomers could induce attached amide oligomers to fold, resulting in hybrid helices.^[48] Herein, we report the design and synthesis of hybrid oligomers **1a**, **1b**, **2**, (*R*)-**3**, and (*S*)-**3**. We demonstrate that, depending on the media, these hybrid backbones can form compact helical conformations through folding of the intrinsically disordered triazole segment(s). These helical conformations are induced by the intrinsically folded state of the amide segment. We also show that the chiral group, introduced at the end of the amide unit of (*R*)-**3** and (*S*)-**3**, is able to induce the whole hybrid backbone to produce a strong helicity bias.

Results and Discussion

Design and synthesis

Hybrid oligomers **1a**, **1b**, **2**, (*R*)-**3**, and (*S*)-**3** have been designed to investigate the possibility of folding-induced folding. For each sequence, a triazole tetramer was used as the intrinsically disordered segment. Previous studies have shown that a folded tetramer, with the H atoms of the triazole rings orientated inward, could form one turn.^[41–43] Compounds **1a** and **1b** contain an amide trimer and pentamer, respectively. It has already been reported that a pentamer of this series is long enough to form one turn,^[33] maximizing homo- or heterogeneous stacking. Thus, a comparison of the folding propensity of the triazole segment of **1a** and **1b** could demonstrate the ability of the folded amide segment to template the folding of the attached triazole segment. Compound **2** contains two triazole segments and was designed to explore the possibility that one folded segment can induce two intrinsically disordered segments to fold. Enantiomers (*R*)-**3** and (*S*)-**3** were prepared to test whether chiral transfer occurs through folding-induced folding. Compounds **4a**, **4b**, (*R*)-**4c**, (*S*)-**4c**, and **5** were used as controls. All of the compounds used in this study are soluble in common organic solvents owing to the presence of aliphatic chains and have been characterized by using ¹H and ¹³C NMR spectroscopy and high-resolution mass spectrometry.

¹H NMR spectroscopy

It is well established that π – π stacking reduces the resolution of ¹H NMR spectra of aromatic molecules. However, ¹H NMR spectroscopy has been used to characterize the folded conformation of linear aromatic sequences.^[49] The ¹H NMR spectra of control compounds **4a** and **5** in CDCl₃ (Figures S82 and S91, see the Supporting Information) and in C₆D₆ (Figure 1 a, b) dis-

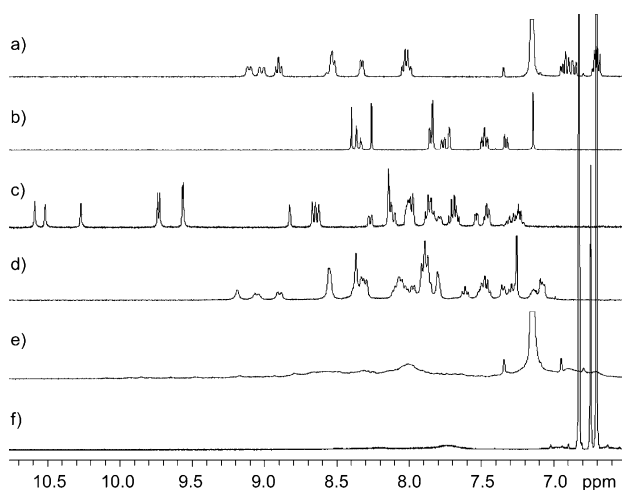


Figure 1. Partial ^1H NMR spectra (400 MHz) of a) **4a** and b) **5** in C_6D_6 , and **1a** in c) $[\text{D}_6]\text{DMSO}$, d) CDCl_3 , e) C_6D_6 , and f) $[\text{D}_8]\text{toluene}$ at 25°C . The concentration was 2.0 mM for all samples.

played high-resolution signals. The ^1H NMR spectra of **1a** in different solvents are also shown in Figure 1. In highly polar $[\text{D}_6]\text{DMSO}$, the ^1H NMR spectrum exhibited sharp signals, indicating flexible conformation of the backbone (Figure 1c). In CDCl_3 , the spectral resolution was good (Figure 1d), but was not as high as that in $[\text{D}_6]\text{DMSO}$, and the resolution was not increased upon dilution (Figure S95, see the Supporting Information). The folded conformation of the amide segment has been well established in chloroform.^[37,38] Therefore, these observations indicate that the conformation of the triazole segment was dominantly flexible in chloroform (Figure 2a, A), but weak intramolecular stacking between the amide and triazole segments also occurred, leading to the formation of a less-stable hybrid helix (Figure 2a, B). The spectra in a $\text{CDCl}_3/\text{C}_6\text{D}_6$ mixture were further recorded with 10% increments of C_6D_6 , revealing

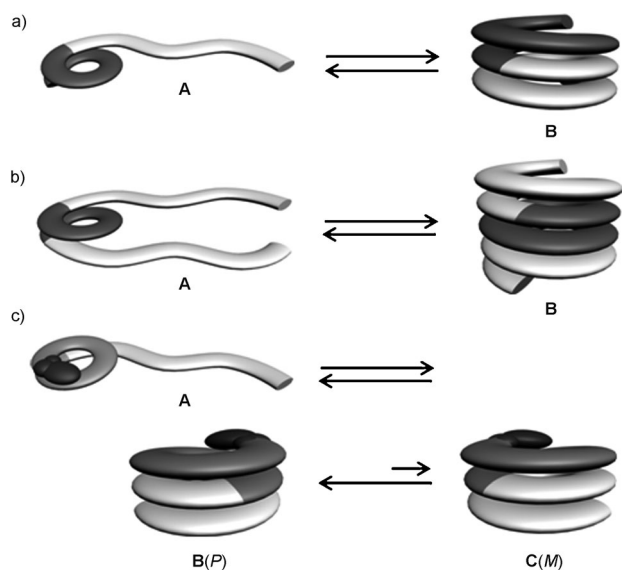


Figure 2. Schematic representation of the solvent-dependent folding-induced folding process of compounds a) **1a** and **1b**, b) **2**, and c) **(S)-3**.

a rapid reduction of the spectral resolution on addition of C_6D_6 (Figure S93, see the Supporting Information). When the percentage of C_6D_6 was increased to approximately 40%, the spectrum only displayed broad unresolved signals. Further increasing the amount of C_6D_6 caused the signals to disappear almost completely. Diluting the solution did not improve the resolution of the spectrum (Figure S95, see the Supporting Information), excluding the possibility that the low resolution was caused by intermolecular stacking. A similar result was also observed in $[\text{D}_8]\text{toluene}$ (Figure 1 f), whereas the ^1H NMR spectra of control compounds **4a** and **5** gave rise to sharp signals, even in pure C_6D_6 . Thus, it is reasonable to propose that the low resolution of the spectra of **1a**, in the binary solvent mixture or in pure C_6D_6 , was caused by the strong intramolecular stacking of the two different aromatic segments, leading to the formation of a relatively stable hybrid helix (Figure 2a, B).^[50] In principle, the triazole segment could adopt two folded patterns, depending on whether the five H atoms of the triazole rings are facing inward or outward. The first pattern could produce a folded entity with a diameter comparable to that of the folded amide oligomers,^[41–43] whereas the diameter of the second folded pattern is substantially larger than that of the amide foldamers.^[47] Thus, the first folded pattern is required to favor intramolecular stacking with the attached amide segment. The spectrum of **1a** in less-polar $[\text{D}_8]\text{toluene}$ did not exhibit any signals, suggesting the formation of a more stable hybrid helix.

The formation of the hybrid helix of **1a** in binary $\text{CDCl}_3/\text{C}_6\text{D}_6$ mixtures or pure C_6D_6 or $[\text{D}_8]\text{toluene}$ may be attributed to several factors. Firstly, compared with that in CDCl_3 or in solvents of higher polarity, the folded conformation of the amide segment in lower polarity media was more compact, increasing the ability to induce the folding of the attached triazole segment through intramolecular stacking. Secondly, the solvophobicity is increased in C_6D_6 or $[\text{D}_8]\text{toluene}$, forcing the triazole segment to fold so that the amount of surface area exposed to the solvent is reduced. Thirdly, the intramolecular stacking between the two connected aromatic segments minimized the surface area of the backbone exposed to the solvent. Finally, in the folded state, the interior region of the amide segment was electronegative because all of the fluorine atoms were directed inward, whereas the external region of the triazole segment was electronegative because the N atoms of the triazole rings were directed outward. As a result, the stacking might be further promoted by intramolecular electrostatic interactions, which become stronger in solvents of low polarity. In highly polar $[\text{D}_6]\text{DMSO}$, the folding-induced folding process should not occur, although the amide trimer might exist in a less-stable folded state (Figure 2a, A) owing to the high stability of the intramolecular N–H...F hydrogen bonding.^[51]

The ^1H NMR spectra of **1b** in different solvents are provided in Figure 3. In contrast to the ^1H NMR spectrum of control compound **4b** (Figure 3a), which gave rise to a set of sharp signals, the spectrum of **1b** in CDCl_3 (Figure 3c) was of low resolution. In C_6D_6 , the signals became even broader (Figure 3b). In contrast, the spectrum in polar $[\text{D}_6]\text{acetone}$ displayed one set of resolved signals (Figure S94, see the Sup-

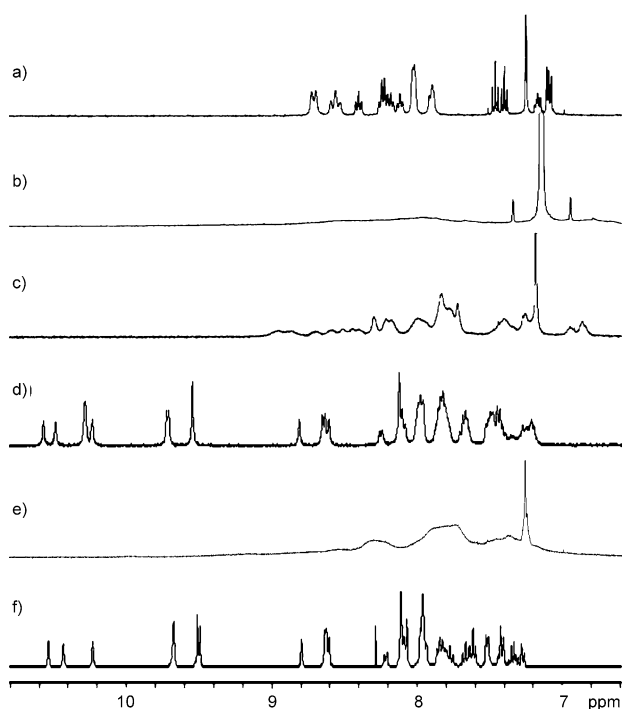


Figure 3. Partial ^1H NMR spectra (400 MHz) of a) **4b** in CDCl_3 ; **1b** in b) C_6D_6 , c) CDCl_3 , and d) $[\text{D}_6]\text{DMSO}$; **2** in e) CDCl_3 and f) $\text{CDCl}_3/[\text{D}_6]\text{DMSO}$ (1:9 v/v) at 25°C . The concentration was 2.0 mM for all samples.

porting Information). Adding $[\text{D}_6]\text{DMSO}$ to the solution of CDCl_3 caused the spectral resolution to improve (Figure S94, see the Supporting Information). Just 4% of $[\text{D}_6]\text{DMSO}$ resulted in the formation of a set of resolved signals in the downfield area. With the addition of more $[\text{D}_6]\text{DMSO}$, the spectral resolution was further increased. In pure $[\text{D}_6]\text{DMSO}$, the spectrum displayed sharp signals (Figure 3d). Again, the resolution of the spectra in CDCl_3 was independent of concentration (Figure S96, see the Supporting Information). Furthermore, cooling the CDCl_3 solution from 40 to -50°C reduced the resolution of the spectra (Figure S98, see the Supporting Information), reflecting the dynamic feature of the helical conformation, which could not be frozen at low temperature. Therefore, the above observations suggest that, in CDCl_3 , **1b** undergoes the folding-induced folding process (Figure 2a, B), demonstrating that the longer folded pentaamide was more powerful than the shorter triamide (**1a**) in inducing the folding of the attached triazole segment. This is not unexpected because the pentamer could produce a one-turn helix, providing the maximum area for stacking with the attached triazole segment. The very broad spectrum in C_6D_6 reflects the formation of a more compact hybrid helix. In $[\text{D}_6]\text{DMSO}$, the triazole segment prefers to exist in disordered states as observed for **1a**.

Encouraged by the above observations, we synthesized compound **2**, in which two triazole segments are attached to a folded amide pentamer. The ^1H NMR spectrum of **2** in CDCl_3 exhibited very broad signals that were independent of concentration (Figure S97, see the Supporting Information). The resolution of this spectrum was lower than that of the shorter compound, **1b**. The ^1H NMR spectra of the reported F–H \cdots N hydro-

gen bonded aromatic amide pentamers or longer heptamers with the same backbone, in CDCl_3 , exhibit a set of sharp signals in the downfield area.^[37a,38] This result suggests that the central folded amide segment of **2** was able to induce the two attached triazole segments to fold, producing a longer hybrid helix through stacking (Figure 2b, B). Upon cooling the solution of **2** in CDCl_3 , from 40 to -50°C , the resolution of the ^1H NMR spectra gradually decreased. These results were similar to those for **1b**, again reflecting the dynamic nature of the helical conformation. Adding $[\text{D}_6]\text{DMSO}$ to the solution remarkably suppressed this process and, in the binary solvent containing 10% $[\text{D}_6]\text{DMSO}$, the spectrum gave rise to a set of resolved signals, indicating the high flexibility of the two triazole segments. Given the stability of N–H \cdots F hydrogen bonding, the folded state of the amide segment should be maintained in this binary medium and the whole backbone produced the unique flexible-folded-flexible conformation (Figure 2b, A). When the content of $[\text{D}_6]\text{DMSO}$ was increased to 90% (Figure S94, see the Supporting Information), the spectrum afforded a set of sharp signals, implying the loss of intramolecular stacking between the two different aromatic segments.

Enantiomers (*R*)-**3** and (*S*)-**3** consist of a tetraamide segment attached to a triazole tetramer and a chiral group. The ^1H NMR spectrum in CDCl_3 exhibited unresolved broad signals, but the spectrum in $[\text{D}_6]\text{DMSO}$ displayed one set of sharp signals. These results are very similar to those observed for **1b** and **2**. In contrast, control compounds (*S*)-**4c** and (*R*)-**4c** afforded a spectrum with high resolution in both solvents. Thus, we propose that, in CDCl_3 , the folded tetraamide segment of (*R*)-**3** and (*S*)-**3** was able to induce the attached triazole segment to fold through intramolecular stacking (Figure 2c). The spectrum of (*R*)-**3** and (*S*)-**3** did not display any signals with good resolution in the downfield area, therefore, we propose that in chloroform or less-polar solvents, the naphthalene unit of (*R*)-**3** and (*S*)-**3** also underwent strong intramolecular stacking to afford chiral helices (Figure 3c, B and C), even though this unit is connected by an sp^3 carbon atom to the aromatic backbone. Circular dichroism experiments showed that the chiral carbon atom in (*R*)-**3** and (*S*)-**3** could induce the new hybrid helices to produce a helicity bias (see below).

^{19}F NMR spectroscopy

The ^{19}F NMR spectra of compounds **1a**, **1b**, **2**, and (*R*)-**3** and control compounds **4a**, **4b**, and (*R*)-**4c** in CDCl_3 are shown in Figure 4. As expected, the spectra of the control compounds displayed sharp signals. The signals in the spectrum of **1a** were slightly broadened compared to those of control compound **4a**. This broadening became more obvious for **1b** and (*R*)-**3**, and remarkably, the spectrum of compound **2** did not display any observable signals. Compared with the corresponding signals of the control compounds, the signals of **1a**, **1b**, and (*R*)-**3** are all shifted downfield ($\Delta\delta = 0.2\text{--}4.7$ ppm, Figure 4). For compounds **1b** and (*R*)-**3** this shift was larger than that for **1a**. These results were in accordance with the above ^1H NMR spectroscopy investigations, supporting the proposal that weak stacking interactions occur between the triazole and

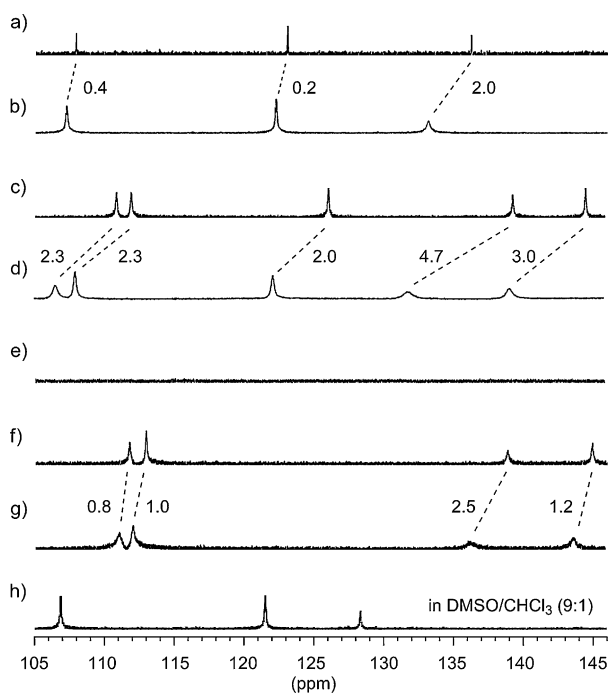


Figure 4. Partial ^{19}F NMR spectrum of a) **4a**, b) **1a**, c) **4b**, d) **1b**, e) **2**, f) (*R*)-**4c**, and g) (*R*)-**3** in CDCl_3 and h) **2** in $[\text{D}_6]\text{DMSO}/\text{CDCl}_3$ (9:1 v/v) at 25°C . The concentration was 2.0 mM for all samples. The data (ppm) indicated are the difference between the chemical shifts of the two related signals. Chemical shifts were referenced to PhCF_3 ($\delta = -62.7$ ppm).

amide segments of **1a**, thus leading to the formation of a less-stable hybrid helix. This stacking interaction was stronger, and the resulting hybrid helices were more stable, for **1b**, **2**, and (*R*)-**3**. The downfield shifting of the ^1H NMR signals of **1b** and (*R*)-**3** can be rationalized by considering that the folded triazole segment imposes an important shielding effect on the fluorine atoms. In $[\text{D}_6]\text{DMSO}$, the spectra of both the control compounds and the target compounds displayed sharp signals and no downfield shifting was observed for the hybrid sequences, indicating that intramolecular stacking of the two different segments did not occur and that the backbones adopted flexible conformations. The fact that the ^{19}F NMR spectrum of **2** in CDCl_3 did not display any observable signals is also consistent with the above ^1H NMR spectroscopy experiments, supporting the formation of a three-segment hybrid helix, which might be facilitated by two factors. Firstly, compound **2** can produce two intramolecular stacking interactions that can promote each other by strengthening the co-planarity of the central amide segment. Secondly, the two-layer stacking of **2** more efficiently reduces the amount of surface area exposed to the solvent, also promoting the formation of the hybrid helix.

UV/Vis spectroscopy

The UV/Vis absorption of linear conjugated molecules is sensitive to conformational change caused by solvophobicity. Solvent titration experiments have been demonstrated as a robust method to investigate the folding of oligomeric aromatic backbones.^[10b,45,52] The above ^1H and ^{19}F NMR spectro-

copy investigations revealed that the hybrid oligomers can undergo intramolecular folding-induced folding, which depends heavily on the polarity of the media. To get more insight into this unique conformational modulation, solvent titration experiments were performed in mixtures of chloroform and *n*-hexane.

UV/Vis dilution experiments showed that for **1a**, **1b**, **2**, and (*R*)-**3** and for control compounds **4a**, **4b**, (*R*)-**4c**, and **5**, the absorption properties obeyed the Beer–Lambert law in chloroform, *n*-hexane, or a 1:1 (v/v) mixture of these solvents, when the concentration was $\leq 5.0 \times 10^{-6}$ M. Titration experiments were then carried out at 5.0×10^{-6} M or a lower concentration to avoid intermolecular stacking (Figure 5). It was found that increasing the percentage of *n*-hexane caused a pronounced hypochromic effect for the four hybrid sequences and also caused a considerable blue shift (up to 15 nm) in the maximum absorbance. However, the trend for each compound was substantially different. For **1a**, the hypochromic effect followed an S curve (Figure 5a). That is, it was initially “dull” and became more intense after the percentage of *n*-hexane was increased to approximately 30%. This observation supports the proposal that, at the early stage, the triazole segment exists

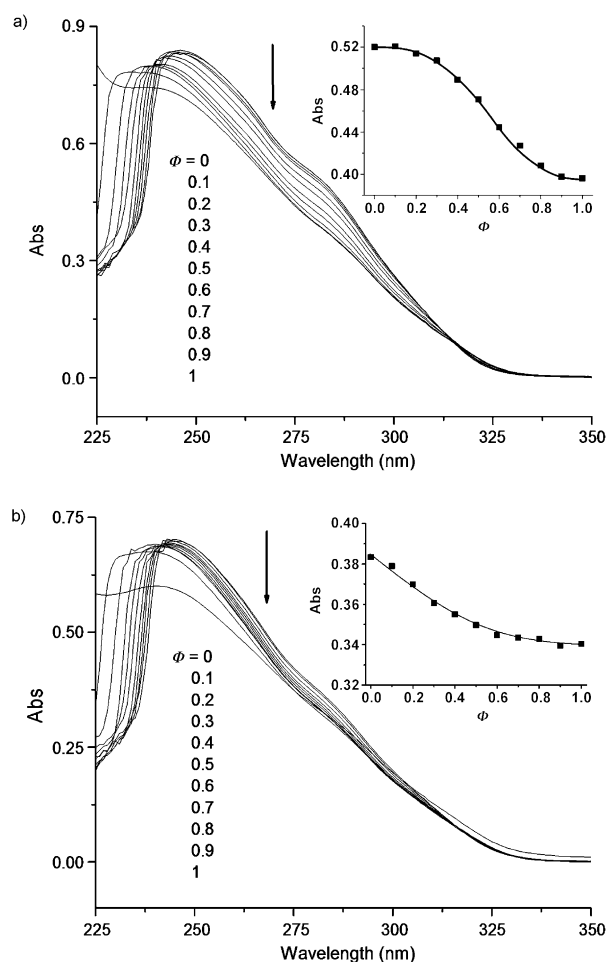


Figure 5. UV/Vis spectra of a) **1a** (5.0×10^{-6} M) and b) **2** (2.5×10^{-6} M) in binary chloroform and *n*-hexane mixtures at 25°C . ϕ represents the relative volume content of *n*-hexane. Inset: The absorbance at 280 nm versus ϕ .

mainly in the flexible state. On increasing the amount of *n*-hexane, the folding and stacking of the attached amide segment were intensified, leading to the formation of the hybrid helix and, consequently, enhanced hypochromism. The hypochromism was reduced when the percentage of *n*-hexane was increased to about 80%, implying that the hybrid helix was close to the maximum stability. Further increasing the *n*-hexane percentage affected the absorbance because of the resulting change in the polarity of the medium. Compounds **1b** (Figure S100, see the Supporting Information), **2** (Figure 5b), and (*R*)-**3** (Figure S101, see the Supporting Information) showed a continuous and smooth hypochromism. On increasing the amount of *n*-hexane, the curve tended to flatten, suggesting that the triazole segment might be approaching folding saturation.

The UV/Vis spectra of 1:1 mixtures of **4a**, **4b**, and (*R*)-**4c** with **5**, at 5.0×10^{-6} M in a mixture of chloroform and *n*-hexane, were also recorded. For all of the mixtures, before the content of *n*-hexane was increased to approximately 70% ($\Phi = 0.7$, Φ represents the relative volume content of *n*-hexane), no important hypochromic effect was observed. On increasing the *n*-hexane content further, the absorbance of the four mixtures showed a notable hypochromic effect. However, similar hypochromism was not observed at lower concentration (1.0×10^{-6} M). At 5.0×10^{-6} M, solutions of pure **4a**, **4b**, (*R*)-**4c**, or **5** did not exhibit similar hypochromism in chloroform, *n*-hexane, or a 1:1 mixture of these solvents. Thus, the hypochromic behavior of the four mixtures, observed at high *n*-hexane content, can be reasonably attributed to intermolecular heterogeneous stacking. Compared with this weak intermolecular stacking, intramolecular stacking of the amide and triazole segments of the hybrid sequences was substantially stronger and could occur in chloroform, which is usually considered as a solvent that weakens aromatic stacking,^[10b,50] or in a mixture of chloroform with benzene or *n*-hexane.

Circular dichroism (CD) spectroscopy

The CD spectra of compounds (*R*)-**3**, (*S*)-**3**, and (*R*)-**4c** in a binary chloroform/*n*-hexane mixture are shown in Figure 6. In pure chloroform, (*R*)-**3** and (*R*)-**4c** both exhibited a negative Cotton effect. Similar signals were not observed for the shorter chiral analogues (compounds (*R*)-**36–38** in the Supporting Information) of (*R*)-**4c**. The maximum CD signal for both chiral molecules was reached at around 295 nm. However, the signal for (*R*)-**3** was substantially stronger than that for (*R*)-**4c**. The CD signal of (*R*)-**3** could be attributed to the helicity bias of the folded backbone, induced by the attached chiral center by intramolecular stacking of the two aromatic segments.^[53]

In the binary chloroform/*n*-hexane mixture, increasing the amount of *n*-hexane (up to $\Phi = 0.5$) remarkably enhanced the signal of (*R*)-**3**. Further increasing the amount of *n*-hexane caused the solution to become turbid, implying that precipitation of (*R*)-**3** occurred. Similar signal enhancement was not observed for (*R*)-**4c**, which instead exhibited a stable CD signal, even when Φ was increased to 0.7. Thus, the signal enhancement observed for (*R*)-**3** reflects the enhanced helicity bias of

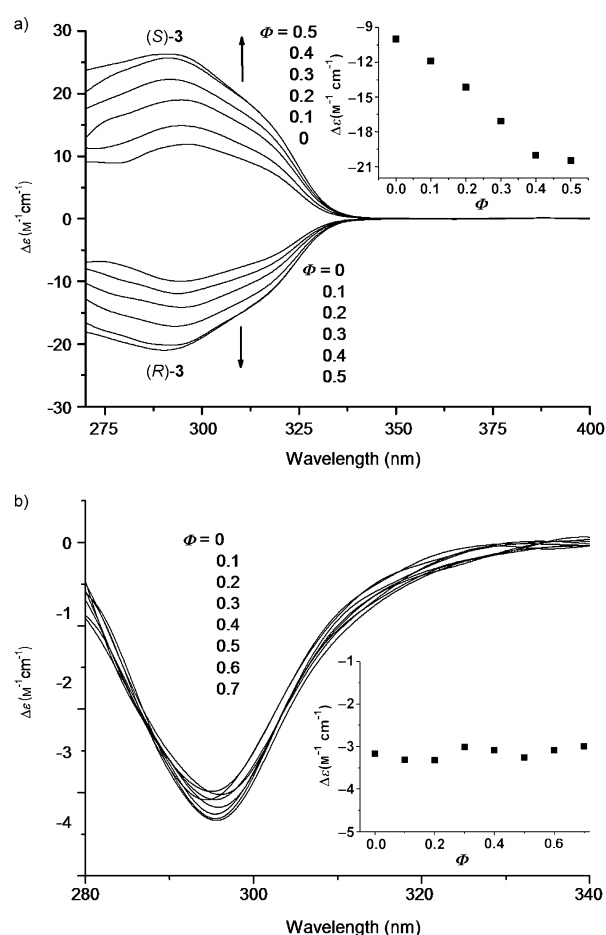


Figure 6. CD spectra of a) enantiomers (*R*)-**3** and (*S*)-**3** and b) (*R*)-**4c** in chloroform/*n*-hexane mixtures at 25 °C (Inset: CD intensity at 295 nm versus Φ). The concentration was 0.3 mM for all samples.

the whole backbone, a result of the enhancement of the intramolecular stacking of the two aromatic segments on decreasing the polarity of the medium (Figure 2c, B and C). This observation was consistent with the above UV/Vis experiments of (*R*)-**3** in the same solvent system (Figure S101, see the Supporting Information). The CD spectra of (*R*)-**3** in chloroform/*n*-hexane ($\Phi = 0.3$) were also recorded at different temperatures. Within the studied temperature range (30 to -16 °C), the CD signal gradually intensified on lowering the temperature (Figure S102, see the Supporting Information), suggesting that the chiral helical conformation becomes more compact at lower temperature. Similar signal enhancement was also observed in a mixture of chloroform with cyclohexane or toluene (Figures S103 and S104, see the Supporting Information). Notably, on increasing the amount of the two less-polar solvents to about 50–60%, the CD signal intensity ceased to increase, implying that compacting of the hybrid helices had reached its maximum. As expected, compound (*S*)-**3** gave rise to a positive Cotton effect, which was also intensified on increasing the amount of *n*-hexane (Figure 6a). For compounds (*R*)-**3**, (*S*)-**3**, and (*R*)-**4c**, in highly polar DMF, no CD signal was observed, indicating that any intramolecular stacking was very weak and that the backbones adopted a flexible conformation. These re-

sults are consistent with the above ^1H and ^{19}F NMR and UV/Vis experiments.

Density functional theory (DFT) calculations

To further understand the conformational change of the new hybrid sequences, M062X DFT calculations were performed in chloroform (for calculation method and details, see the Supporting Information) with Gaussian 09 package using the 6-31 G(d,p) basis set for compounds **1b**, **2**, and (*S*)-**3** in chloroform. To simplify the calculations, we first carried out Monte Carlo conformational searches for the aromatic amide segment of these compounds, with the side chains being omitted, to obtain the energy minimum folded conformation. The backbones were then constructed by attaching one (for **1b** and (*S*)-**3**) or two (for **2**) randomly arranged flexible triazole segments to the corresponding folded aromatic amide segment. These partially compact sequences were, again, subjected to conformational searches. In total, 5000 structures were accumulated and the ten lowest-energy conformers were further optimized. The representative conformers are shown in Figure 7.

For all three compounds (**1b**, **2**, and (*S*)-**3**), the fully helical conformer, in which the amide and triazole segments are stacked intramolecularly, was the lowest-energy conformer. As expected, the two different folded segments in these conformers were comparable in diameter and thus were well matched for stacking. Both folded segments formed one turn, maximizing the stacking ability. The distance between the stacking aromatic units was in the range of 3.4–3.5 Å,^[54] which is typical for this kind of noncovalent interaction. For **1b**, there were several different low-energy conformers, in which the amide segment folded and the triazole segment was flexible. The free energies of these conformers were similar, and the conformer with the lowest energy (Figure 7a) was 17.6 kcal mol⁻¹ higher in energy than the fully folded conformer (Figure 7b). For compound **2**, the free energy of the conformers (Figure 7d, e) with either one or none of the triazole segments stacking with the central amide segment is either 29.6 or 57.1 kcal mol⁻¹ higher than that of the fully folded conformer (Figure 7c), respectively. The second value is approximately double that of the first one, indicating that stabilization, caused by the intramolecular stacking between the two different kinds of aromatic segments, increases as the stacking aromatic units are increased. In principle, the fully folded (*S*)-**3** results in two helical diastereoisomers,^[55] that is, the right-handed conformer (*S*)-*P* and the left-handed conformer (*S*)-*M* (Figure 2c, B and C). DFT calculations revealed that the *P* conformer (Figure 7f) was 9.8 kcal mol⁻¹ lower in free energy than the *M* conformer (Figure 7g), suggesting that (*S*)-**3** exists mainly as the *P* diastereoisomeric conformer. These calculations also revealed that for conformers of (*S*)-**3** with the triazole segment being disordered the energies were generally higher than the corresponding fully folded conformers. For the (*S*)-*P* series, the energy of the conformer that has a folded amide segment and a flexible triazole segment (Figure 7h) was at least 12.5 kcal mol⁻¹ higher than that of the fully folded conformer (Figure 7f).

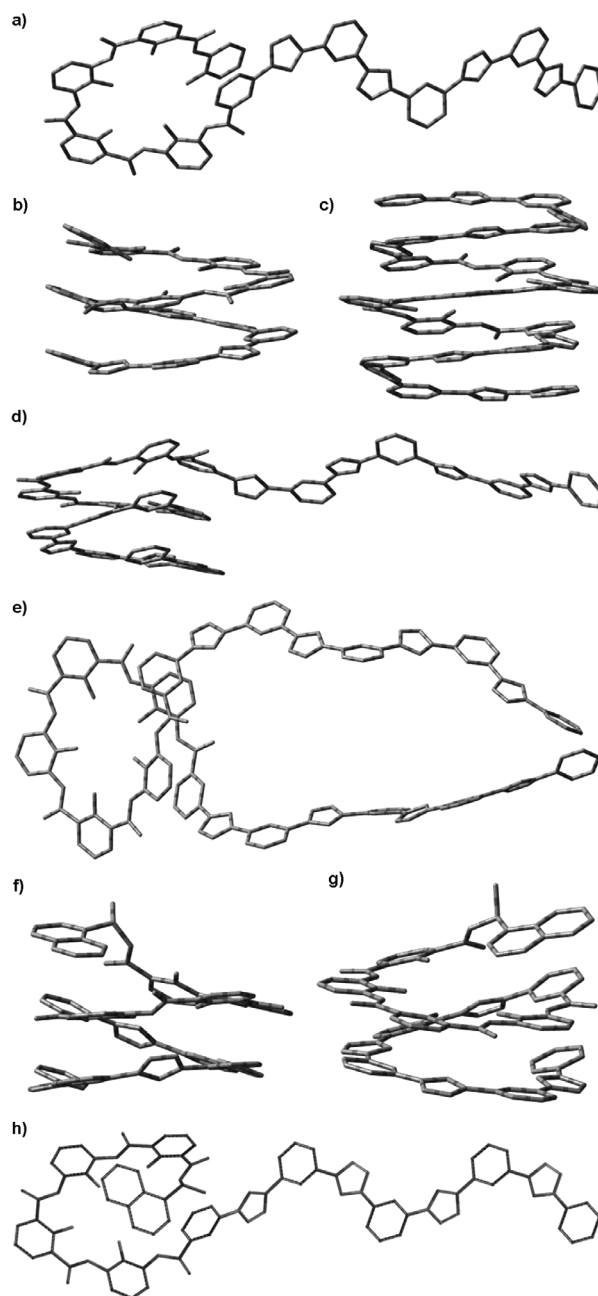


Figure 7. The optimized conformers of hybrid oligomers that have a folded amide segment and one or two folded or disordered triazole segments, calculated in chloroform with Gaussian 09 package using the 6-31 G(d) basis set. For **1b**: the triazole segment was a) disordered and b) folded; For **2**: c) the two triazole segments were folded, d) one triazole was folded and another was disordered, and e) both triazole segments were disordered; For (*S*)-**3**: f) the triazole segment was folded with *P* helicity, g) the triazole segment was folded with *M* helicity, and h) the triazole segment was disordered with *P* helicity.

Conclusion

We have demonstrated that attaching intrinsically disordered aromatic triazole tetramers to hydrogen-bonding-induced folded aromatic oligoamides can lead to folding of the triazole segment(s) through intramolecular stacking between the two different kinds of aromatic segments. In a broad sense, this

folding-induced folding process may be considered as a special binding behavior and, thus, to some extent, resembles the binding-induced folding phenomenon that commonly occurs for natural peptides and proteins. The process is highly dependent on the polarity of the solvents. In solvents of high polarity, the folded conformation of the aromatic amide segment is less stable and, therefore, cannot efficiently induce the folding of the triazole segment. In less-polar solvents, the stable folded state serves well as a compact platform, which, together with the enhanced solvophobic interaction, is able to induce the folding of the attached triazole segment(s). This templating can be very efficient and a chiral center, attached to the end of the folded amide segment, could induce the whole hybrid framework to produce a strong helicity bias.

The successful induction of the folded conformation of one and two intrinsically disordered aromatic triazole oligomer(s) by an attached folded aromatic amide segment raises several issues that we believe are worthy of further study: 1) Is this inducing process a general behavior for aromatic hybrid sequences? 2) Can a short folded segment serve as a "seed" to induce one or two attached polymeric backbones to fold and to further transfer and amplify the chirality to the whole polymeric backbone? A systematic exploration of these possibilities may lead to the development of functional helices or polymeric tubes that are potentially useful for advanced recognition, encapsulation, or transport.

Acknowledgements

We are grateful to the Ministry of Science and Technology (2013CB834501), the Ministry of Education (IRT1117), and the National Natural Science Foundation of China (21272042, 21102019), and to the Science and Technology Commission of Shanghai Municipality (13M1400200) for financial support.

Keywords: foldamers · helices · hydrogen bonding · stacking · triazoles

- [1] D. L. Nelson, M. M. Cox, *Lehninger's Principles of Biochemistry*, 5th ed., W. H. Freeman & Company, New York, **2008**.
- [2] V. N. Uversky, *J. Mol. Biol.* **2012**, *418*, 267–267.
- [3] Y.-J. Chen, M. Inouye, *Curr. Opin. Struct. Biol.* **2008**, *18*, 765–770.
- [4] J. Montreuil, J. F. G. Vliegthart, H. Schachter, *Glycoproteins*, Elsevier, Amsterdam, **1995**.
- [5] J. A. Speir, J. E. Johnson, *Curr. Opin. Struct. Biol.* **2012**, *22*, 65–71.
- [6] S. Hecht, I. Huc, *Foldamers: Structure, Properties and Applications*, Wiley-VCH, Weinheim, **2007**.
- [7] D. Seebach, J. L. Matthews, *Chem. Commun.* **1997**, 2015–2022.
- [8] a) S. H. Gellman, *Acc. Chem. Res.* **1998**, *31*, 173–180; b) W. S. Horne, S. H. Gellman, *Acc. Chem. Res.* **2008**, *41*, 1399–1408.
- [9] J. S. Nowick, *Acc. Chem. Res.* **2008**, *41*, 1319–1330.
- [10] a) D. J. Hill, M. J. Mio, R. B. Prince, T. S. Hughes, J. S. Moore, *Chem. Rev.* **2001**, *101*, 3893–4011; b) M. T. Stone, J. M. Heemstra, J. S. Moore, *Acc. Chem. Res.* **2006**, *39*, 11–20.
- [11] M. S. Cubberley, B. L. Iverson, *Curr. Opin. Chem. Biol.* **2001**, *5*, 650–653.
- [12] a) R. P. Cheng, S. H. Gellman, W. F. DeGrado, *Chem. Rev.* **2001**, *101*, 3219–3232; b) C. M. Goodman, S. Choi, S. Shandler, W. F. DeGrado, *Nat. Chem. Biol.* **2007**, *3*, 252–262.
- [13] a) I. Huc, *Eur. J. Org. Chem.* **2004**, 17–29; b) G. Guichard, I. Huc, *Chem. Commun.* **2011**, *47*, 5933–5941.
- [14] a) B. Gong, *Acc. Chem. Res.* **2008**, *41*, 1376–1386; b) K. Yamato, M. Kline, B. Gong, *Chem. Commun.* **2012**, *48*, 12142–12158.
- [15] G. Licini, L. J. Prins, P. Scrimin, *Eur. J. Org. Chem.* **2005**, 969–977.
- [16] a) X. Li, D. Yang, *Chem. Commun.* **2006**, 3367–3379; b) X. Li, Y.-D. Wu, D. Yang, *Acc. Chem. Res.* **2008**, *41*, 1428–1438.
- [17] Y. Zhao, *Curr. Opin. Colloid Interface Sci.* **2007**, *12*, 92–97.
- [18] Y.-D. Wu, W. Han, D.-P. Wang, Y. Gao, Y.-W. Zhao, *Acc. Chem. Res.* **2008**, *41*, 1418–1427.
- [19] I. Saraogi, A. D. Hamilton, *Chem. Soc. Rev.* **2009**, *38*, 1726–1743.
- [20] H. Juwarker, J.-m. Suk, K.-S. Jeong, *Chem. Soc. Rev.* **2009**, *38*, 3316–3325.
- [21] a) Q. Gan, Y. Wang, H. Jiang, *Curr. Org. Chem.* **2011**, *15*, 1293–1301; b) Q. Gan, Y. Ferrand, C. Bao, B. Kauffmann, A. Grélard, H. Jiang, I. Huc, *Science* **2011**, *331*, 1172–1175; c) C. Bao, Q. Gan, B. Kauffmann, H. Jiang, I. Huc, *Chem. Eur. J.* **2009**, *15*, 11530–11536.
- [22] A. Roy, P. Prabhakaran, P. K. Baruah, G. J. Sanjayan, *Chem. Commun.* **2011**, *47*, 11593–11611.
- [23] a) Z.-T. Li, J.-L. Hou, C. Li, *Acc. Chem. Res.* **2008**, *41*, 1343–1353; b) D.-W. Zhang, X. Zhao, J.-L. Hou, Z.-T. Li, *Chem. Rev.* **2012**, *112*, 5271–5316; c) X. Zhao, Z.-T. Li, *Chem. Commun.* **2010**, *46*, 1601–1616.
- [24] a) T. L. Raguse, J. R. Lai, P. R. Le Plae, S. H. Gellman, *Org. Lett.* **2001**, *3*, 3963–3966; b) M. W. Giuliano, W. S. Horne, S. H. Gellman, *J. Am. Chem. Soc.* **2009**, *131*, 9860–9861; c) J. L. Price, E. B. Hadley, J. D. Steinkruger, S. H. Gellman, *Angew. Chem.* **2010**, *122*, 378–381; *Angew. Chem. Int. Ed.* **2010**, *49*, 368–371.
- [25] T. S. Burkoth, E. Beausoleil, S. Kaur, D. Tang, F. E. Cohen, R. N. Zuckermann, *Chem. Biol.* **2002**, *9*, 647–654.
- [26] a) V. Maurizot, C. Dolain, Y. Leydet, J.-M. Léger, P. Guionneau, I. Huc, *J. Am. Chem. Soc.* **2004**, *126*, 10049–10052; b) N. Delsuc, M. Hutin, V. E. Campbell, B. Kauffmann, J. R. Nitschke, I. Huc, *Chem. Eur. J.* **2008**, *14*, 7140–7143; c) N. Delsuc, S. Massip, J.-M. Léger, B. Kauffmann, I. Huc, *J. Am. Chem. Soc.* **2011**, *133*, 3165–3172.
- [27] E. J. Petersson, A. Schepartz, *J. Am. Chem. Soc.* **2008**, *130*, 821–823.
- [28] O. Khakshoor, B. Demeler, J. S. Nowick, *J. Am. Chem. Soc.* **2007**, *129*, 5558–5569.
- [29] a) H.-Y. Hu, J.-F. Xiang, Y. Yang, C.-F. Chen, *Org. Lett.* **2008**, *10*, 69–72; b) H.-Y. Hu, J.-F. Xiang, C.-F. Chen, *Org. Biomol. Chem.* **2009**, *7*, 2534–2539.
- [30] T. A. Martinek, F. Fülöp, *Chem. Soc. Rev.* **2012**, *41*, 687–702.
- [31] a) C. Dolain, C. Zhan, J.-M. Léger, L. Daniels, I. Huc, *J. Am. Chem. Soc.* **2005**, *127*, 2400–2401; b) H.-P. Yi, J. Wu, K.-L. Ding, X.-K. Jiang, Z.-T. Li, *J. Org. Chem.* **2007**, *72*, 870–877; c) R. A. Smaldone, J. S. Moore, *Chem. Eur. J.* **2008**, *14*, 2650–2657; d) K. Srinivas, B. Kauffmann, C. Dolain, J.-M. Léger, L. Ghoséz, I. Huc, *J. Am. Chem. Soc.* **2008**, *130*, 13210–13211; e) M. M. Müller, M. A. Windsor, W. C. Pomerantz, S. H. Gellman, D. Hilvert, *Angew. Chem.* **2009**, *121*, 940–943; *Angew. Chem. Int. Ed.* **2009**, *48*, 922–925; f) H. Cho, Z. Zhong, Y. Zhao, *Tetrahedron* **2009**, *65*, 7311–7316; g) G. Maayan, M. D. Ward, K. Kirshenbaum, *Proc. Natl. Acad. Sci. USA* **2009**, *106*, 13679–13684; h) R. R. Araghi, B. Kocsch, *Chem. Commun.* **2011**, *47*, 3544–3546.
- [32] a) H. Jiang, J.-M. Léger, P. Guionneau, I. Huc, *Org. Lett.* **2004**, *6*, 2985–2988; b) L. Yuan, W. Feng, K. Yamato, A. R. Sanford, D. Xu, H. Guo, B. Gong, *J. Am. Chem. Soc.* **2004**, *126*, 11120–11121; c) J. Zhu, X.-Z. Wang, Y.-Q. Chen, X.-K. Jiang, X.-Z. Chen, Z.-T. Li, *J. Org. Chem.* **2004**, *69*, 6221–6227; d) F. Li, Q. Gan, L. Xue, Z.-m. Wang, H. Jiang, *Tetrahedron Lett.* **2009**, *50*, 2367–2369.
- [33] a) B. Qin, X. Chen, X. Fang, Y. Shu, Y. K. Yip, Y. Yan, S. Pan, W. Q. Ong, C. Ren, H. Su, H. Zeng, *Org. Lett.* **2008**, *10*, 5127–5130; b) B. Qin, W. Q. Ong, R. Ye, Z. Du, X. Chen, Y. Yan, K. Zhang, H. Su, H. Zeng, *Chem. Commun.* **2011**, *47*, 5419–5421; c) C. Ren, V. Maurizot, H. Zhao, J. Shen, F. Zhou, W. Q. Ong, Z. Du, K. Zhang, H. Su, H. Zeng, *J. Am. Chem. Soc.* **2011**, *133*, 13930–13933; d) H. Fu, Y. Liu, H. Zeng, *Chem. Commun.* **2013**, *49*, 4127–4144; e) W. Q. Ong, H. Zeng, *J. Inclusion Phenom. Macrocyclic Chem.* **2013**, *76*, 1–11; f) H. Zhao, W. Q. Ong, F. Zhou, X. Fang, X. Chen, S. F. Y. Li, H. Su, N.-J. Cho, H. Zeng, *Chem. Sci.* **2012**, *3*, 2042–2046.
- [34] a) Z.-M. Shi, J. Huang, Z. Ma, Z. Guan, Z.-T. Li, *Macromolecules* **2010**, *43*, 6185–6192; b) K.-D. Zhang, X. Zhao, G.-T. Wang, Y. Liu, Y. Zhang, H.-J. Lu, X.-K. Jiang, Z.-T. Li, *Angew. Chem.* **2011**, *123*, 10040–10044; *Angew. Chem. Int. Ed.* **2011**, *50*, 9866–9870.

- [35] a) H. Yin, A. D. Hamilton, *Angew. Chem.* **2005**, *117*, 4200–4235; *Angew. Chem. Int. Ed.* **2005**, *44*, 4130–4163; b) C. G. Cummings, A. D. Hamilton, *Curr. Opin. Chem. Biol.* **2010**, *14*, 341–346; c) M. J. Adler, A. G. Jamieson, A. D. Hamilton, *Curr. Top. Microbiol. Immunol.* **2011**, *348*, 1–23; d) A. D. Bautista, C. J. Craig, E. A. Harker, A. Schepartz, *Curr. Opin. Chem. Biol.* **2007**, *11*, 685–692; e) G. N. Tew, R. W. Scott, M. L. Klein, W. F. DeGrado, *Acc. Chem. Res.* **2010**, *43*, 30–39; f) V. Azzarito, K. Long, N. S. Murphy, A. J. Wilson, *Nat. Chem.* **2013**, *5*, 161–173.
- [36] a) J. D. Sadowsky, M. A. Schmitt, H.-S. Lee, N. Umezawa, S. Wang, Y. Tomita, S. H. Gellman, *J. Am. Chem. Soc.* **2005**, *127*, 11966–11968; b) W. S. Horne, L. M. Johnson, T. J. Ketas, P. J. Klasse, M. Lu, J. P. Moore, S. H. Gellman, *Proc. Natl. Acad. Sci. USA* **2009**, *106*, 14751–14756; c) L. Delaurière, Z. Dong, K. Laxmi-Reddy, F. Godde, J.-J. Toulmé, I. Huc, *Angew. Chem.* **2012**, *124*, 488–492; *Angew. Chem. Int. Ed.* **2012**, *51*, 473–477.
- [37] a) C. Li, S.-F. Ren, J.-L. Hou, H.-P. Yi, S.-Z. Zhu, X.-K. Jiang, Z.-T. Li, *Angew. Chem.* **2005**, *117*, 5871–5875; *Angew. Chem. Int. Ed.* **2005**, *44*, 5725–5729; b) Y.-Y. Zhu, J. Wu, C. Li, J. Zhu, J.-L. Hou, C.-Z. Li, X.-K. Jiang, Z.-T. Li, *Cryst. Growth Des.* **2007**, *7*, 1490–1496.
- [38] a) C. Li, Y.-Y. Zhu, H.-P. Yi, C.-Z. Li, X.-K. Jiang, Z.-T. Li, Y.-H. Yu, *Chem. Eur. J.* **2007**, *13*, 9990–9998; b) Y.-Y. Zhu, C. Li, G.-Y. Li, X.-K. Jiang, Z.-T. Li, *J. Org. Chem.* **2008**, *73*, 1745–1751; c) L. Wang, Z.-Y. Xiao, J.-L. Hou, G.-T. Wang, X.-K. Jiang, Z.-T. Li, *Tetrahedron* **2009**, *65*, 10544–10551.
- [39] Q. Gan, C. Bao, B. Kauffmann, A. Grelard, J. Xiang, S. Liu, I. Huc, H. Jiang, *Angew. Chem.* **2008**, *120*, 1739–1742; *Angew. Chem. Int. Ed.* **2008**, *47*, 1715–1718.
- [40] a) C. Ren, S. Xu, J. Xu, H. Chen, H. Zeng, *Org. Lett.* **2011**, *13*, 3840–3843; b) C. Ren, F. Zhou, B. Qin, R. Ye, S. Shen, H. Su, H. Zeng, *Angew. Chem.* **2011**, *123*, 10800–10803; *Angew. Chem. Int. Ed.* **2011**, *50*, 10612–10615.
- [41] a) Y. Hua, A. H. Flood, *Chem. Soc. Rev.* **2010**, *39*, 1262–1271; b) K. P. McDonald, Y. Hua, A. H. Flood, *Top. Heterocycl. Chem.* **2010**, *24*, 341–366; c) S. Lee, A. H. Flood, *Top. Heterocycl. Chem.* **2012**, *28*, 85–107; d) Y. Li, A. H. Flood, *J. Am. Chem. Soc.* **2008**, *130*, 12111–12122; e) Y. Hua, A. H. Flood, *J. Am. Chem. Soc.* **2010**, *132*, 12838–12840; f) K. P. McDonald, R. O. Ramabhadran, S. Lee, K. Raghavachari, A. H. Flood, *Org. Lett.* **2011**, *13*, 6260–6263.
- [42] a) H. Juwarker, J. M. Lenhardt, D. M. Pham, S. L. Craig, *Angew. Chem.* **2008**, *120*, 3800–3803; *Angew. Chem. Int. Ed.* **2008**, *47*, 3740–3743; b) H. Juwarker, J. M. Lenhardt, J. C. Castillo, E. Zhao, S. Krishnamurthy, R. M. Jamiolkowski, K.-H. Kim, S. L. Craig, *J. Org. Chem.* **2009**, *74*, 8924–8934.
- [43] R. M. Meudtner, S. Hecht, *Angew. Chem.* **2008**, *120*, 5004–5008; *Angew. Chem. Int. Ed.* **2008**, *47*, 4926–4930.
- [44] a) Y. Wang, F. Bie, H. Jiang, *Org. Lett.* **2010**, *12*, 3630–3633; b) Y. Wang, J. Xiang, H. Jiang, *Chem. Eur. J.* **2011**, *17*, 613–619.
- [45] Y. Wang, F. Li, Y. Han, F. Wang, H. Jiang, *Chem. Eur. J.* **2009**, *15*, 9424–9433.
- [46] D. Zornik, R. M. Meudtner, T. El Malah, C. M. Thiele, S. Hecht, *Chem. Eur. J.* **2011**, *17*, 1473–1484.
- [47] L.-Y. You, S.-G. Chen, X. Zhao, Y. Liu, W.-X. Lan, Y. Zhang, H.-J. Lu, C.-Y. Cao, Z.-T. Li, *Angew. Chem.* **2012**, *124*, 1689–1693; *Angew. Chem. Int. Ed.* **2012**, *51*, 1657–1661.
- [48] a) D. Sánchez-García, B. Kauffmann, T. Kawanami, H. Ihara, M. Takafuji, M.-H. Delville, I. Huc, *J. Am. Chem. Soc.* **2009**, *131*, 8642–8648; b) M. Kudo, V. Maurizot, B. Kauffmann, A. Tanatani, I. Huc, *J. Am. Chem. Soc.* **2013**, *135*, 9628–9631.
- [49] J. C. Nelson, J. G. Saven, J. S. Moore, P. G. Wolynes, *Science* **1997**, *277*, 1793–1796.
- [50] C. R. Martinez, B. L. Iverson, *Chem. Sci.* **2012**, *3*, 2191–2201.
- [51] J. F. Galan, J. Brown, J. L. Wildin, Z. Liu, D. Liu, G. Moyna, V. Pophristic, *J. Phys. Chem. B* **2009**, *113*, 12809–12815.
- [52] J.-L. Hou, X.-B. Shao, G.-J. Chen, Y.-X. Zhou, X.-K. Jiang, Z.-T. Li, *J. Am. Chem. Soc.* **2004**, *126*, 12386–12394.
- [53] M. T. Stone, J. M. Fox, J. S. Moore, *Org. Lett.* **2004**, *6*, 3317–3320.
- [54] a) R. Podeszwa, R. Bukowski, K. Szalewicz, *J. Phys. Chem. A* **2006**, *110*, 10345–10354; b) J. G. Hill, J. A. Platts, H.-J. Werner, *Phys. Chem. Chem. Phys.* **2006**, *8*, 4072–4078.
- [55] C. Dolain, H. Jiang, J.-M. Léger, P. Guionneau, I. Huc, *J. Am. Chem. Soc.* **2005**, *127*, 12943–12591.

Received: October 24, 2013

Published online on January 2, 2014